Electronic Supplementary Material (ESI) for Polymer Chemistry.

Supplementary Information

Boron Difluoride Formazanate Copolymers with 9,9-Di-*n*-hexylfluorene Prepared by Copper Catalyzed Alkyne-Azide Cycloaddition Chemistry

*Stephanie M. Barbon and Joe B. Gilroy**

Department of Chemistry and the Centre for Advanced Materials and Biomaterials Research (CAMBR), The University of Western Ontario, 1151 Richmond St. N., London, Ontario, Canada, N6A 5B7. Tel: +1-519-661-2111 ext. 81561; E-mail: joe.gilroy@uwo.ca

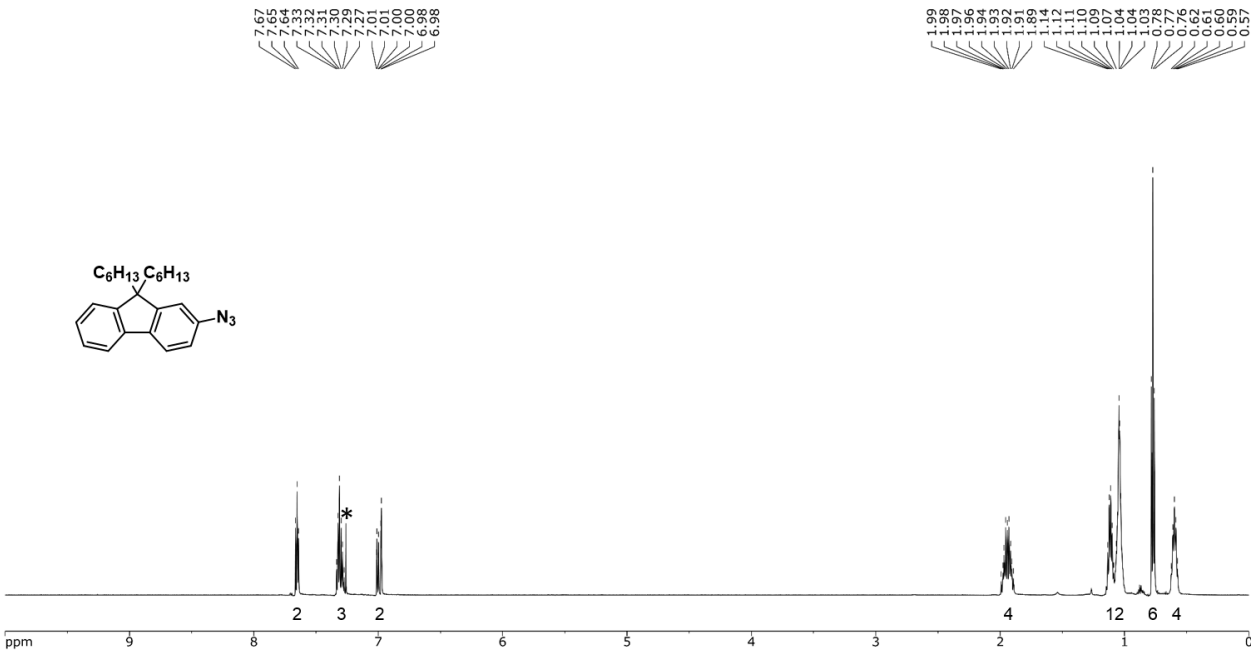

Fig. S1 ^{1}H NMR spectrum of **(hex$_2$Fl)N$_3$** in $CDCl_3$. The asterisk denotes residual solvent signal.

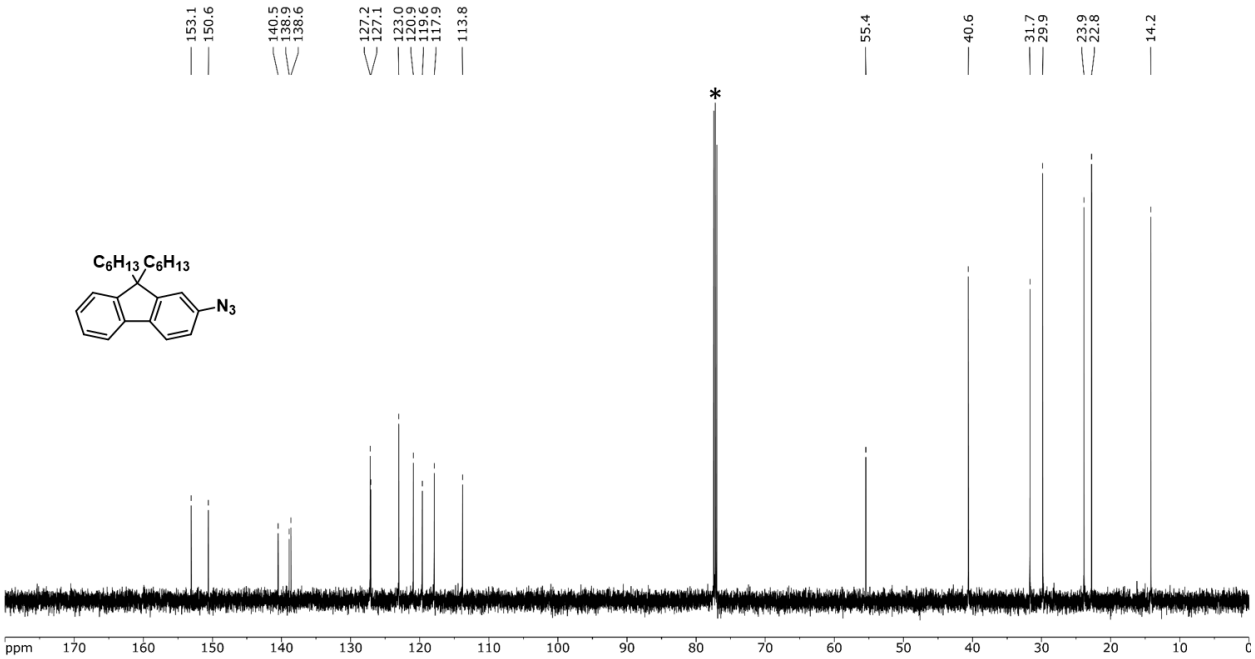

Fig. S2 $^{13}C\{^{1}H\}$ NMR spectrum of **(hex$_2$Fl)N$_3$** in $CDCl_3$. The asterisk denotes solvent signal.

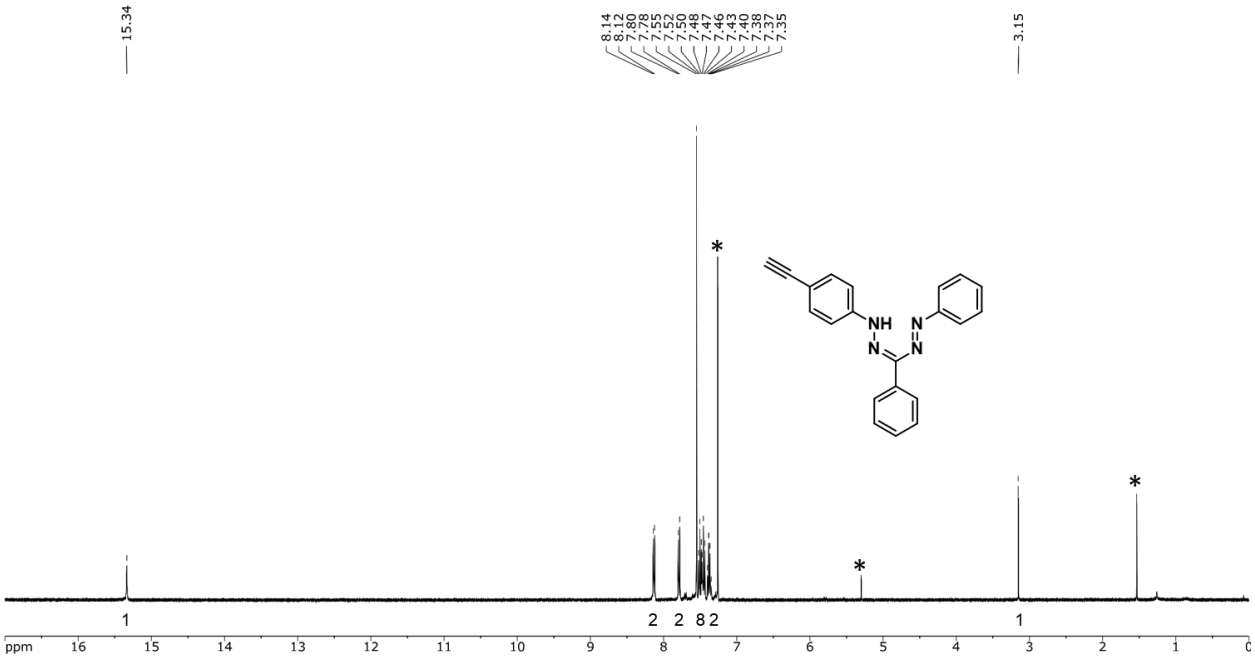

Fig. S3 ^{1}H NMR spectrum of **HC_2(LH)** in $CDCl_3$. The asterisks denote residual solvent signals.

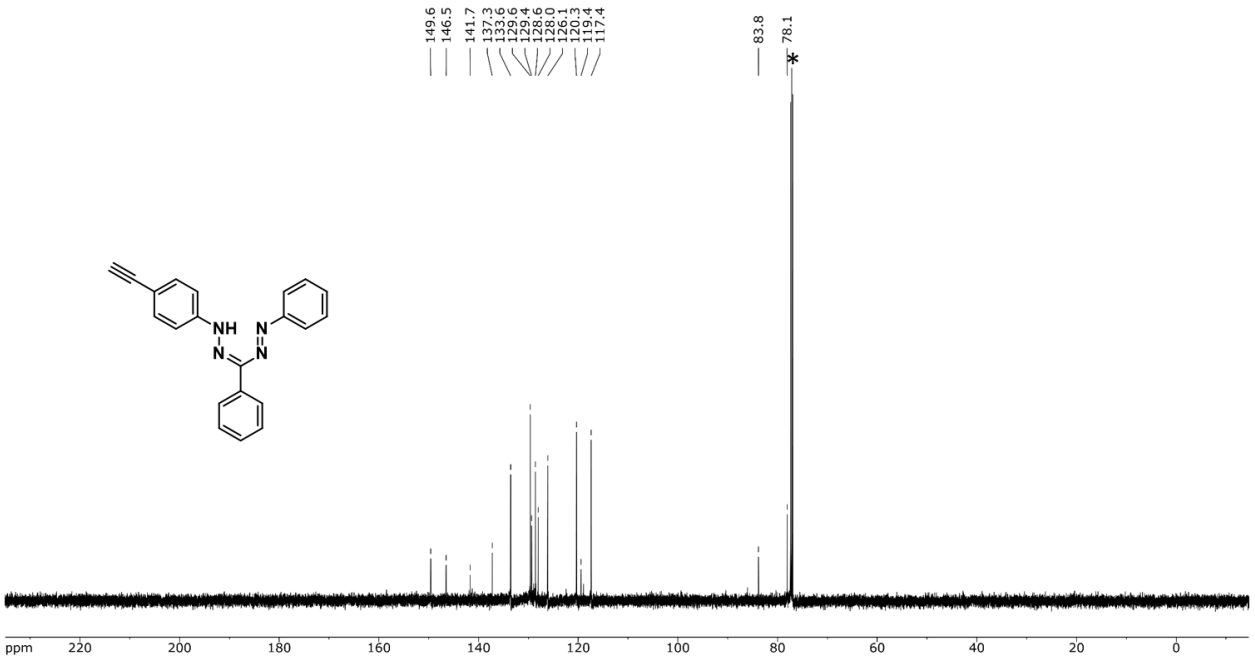

Fig. S4 $^{13}C\{^{1}H\}$ NMR spectrum of **HC_2(LH)** in $CDCl_3$. The asterisk denotes solvent signal.

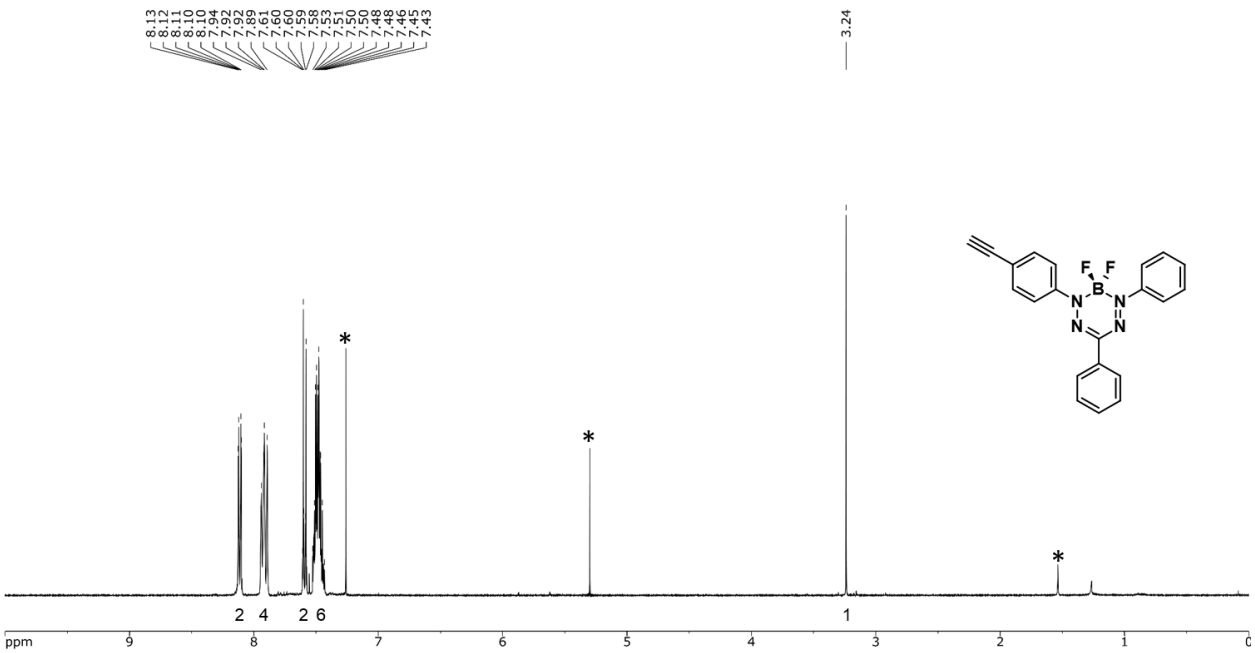

Fig. S5 ^{1}H NMR spectrum of **$HC_2(BF_2L)$** in $CDCl_3$. The asterisks denote residual solvent signals.

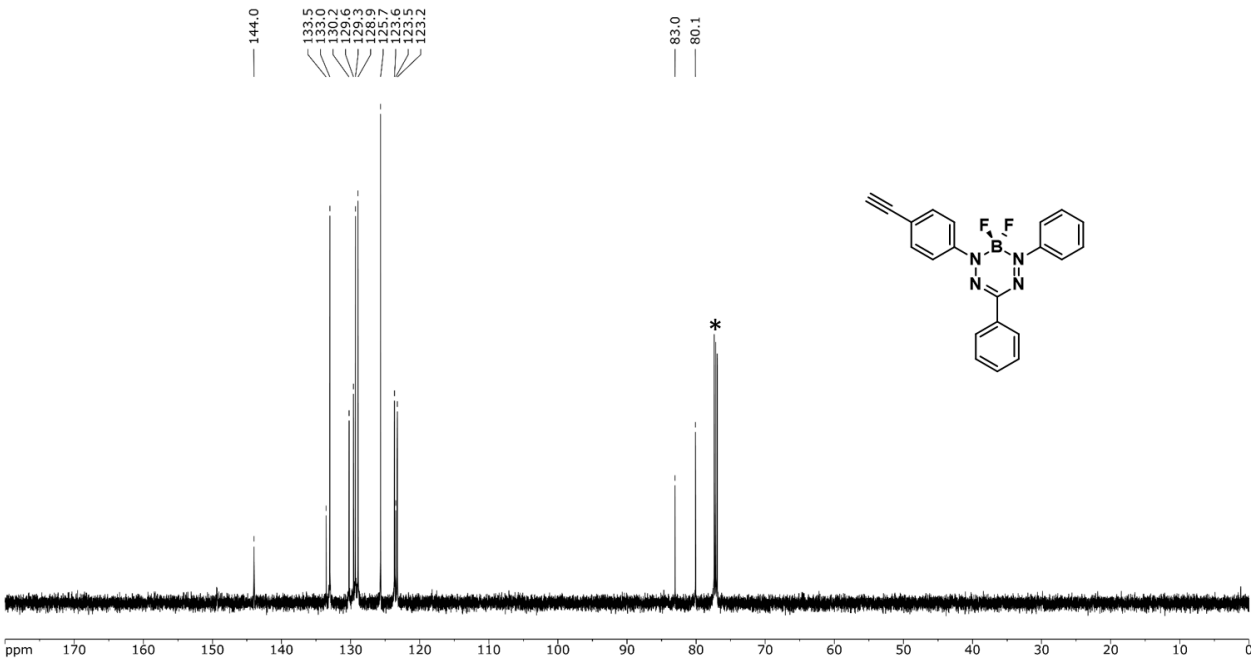

Fig. S6 $^{13}C\{^{1}H\}$ NMR spectrum of **$HC_2(BF_2L)$** in $CDCl_3$. The asterisk denotes solvent signal.

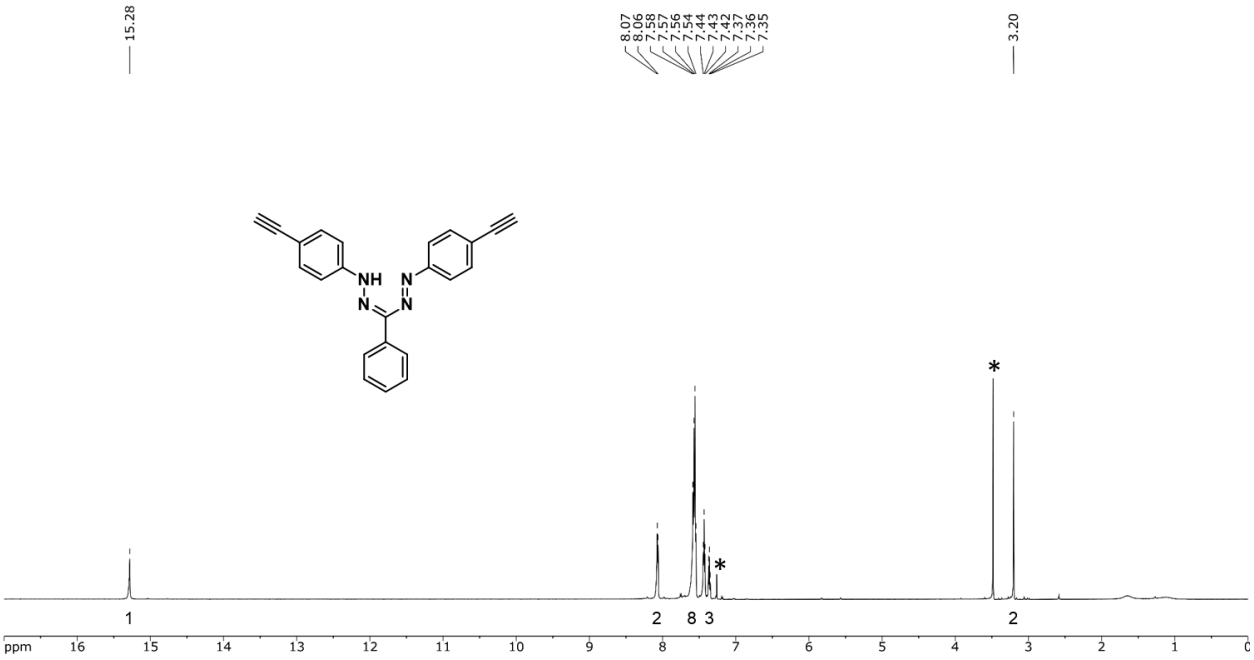

Fig. S7 ^{1}H NMR spectrum of **$HC_2(LH)C_2H$** in $CDCl_3$. The asterisks denote residual solvent signals.

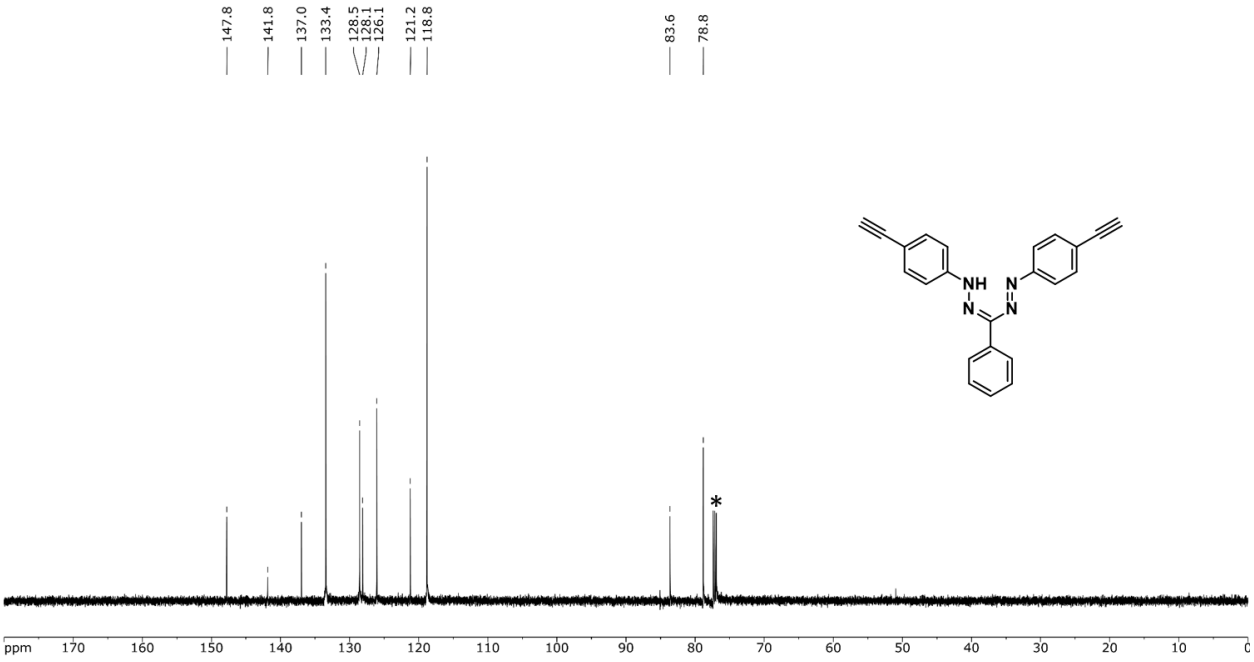

Fig. S8 $^{13}C\{^{1}H\}$ NMR spectrum of **$HC_2(LH)C_2H$** in $CDCl_3$. The asterisk denotes solvent signal.

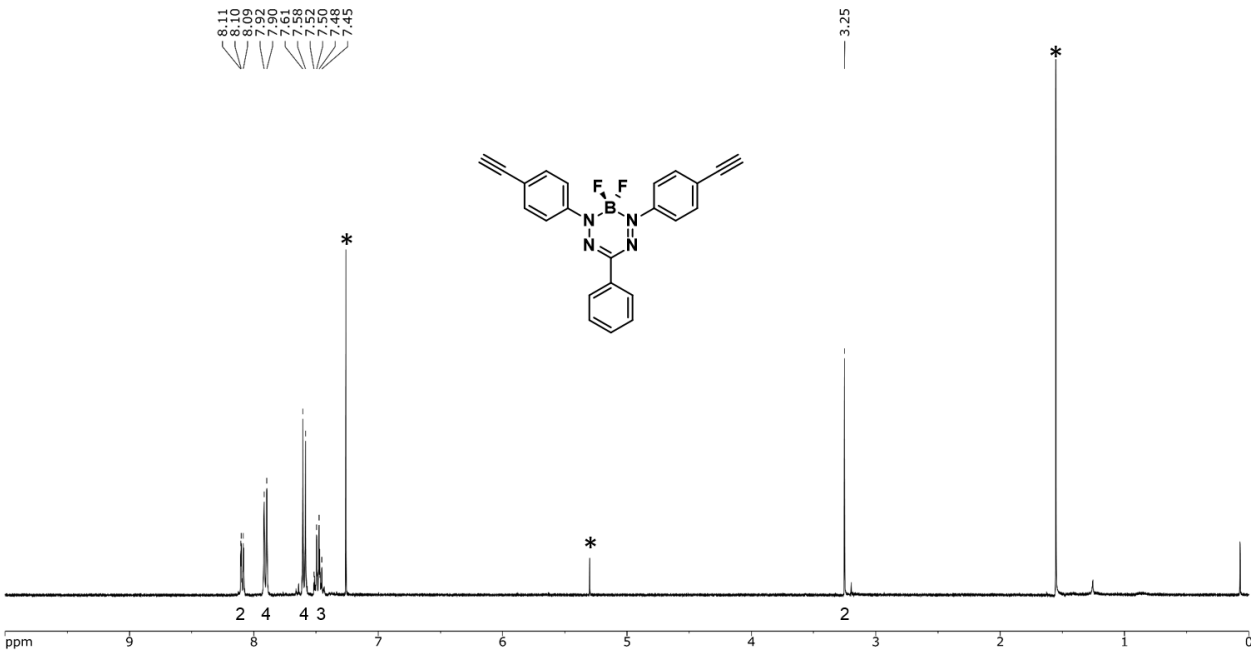

Fig. S9 ^{1}H NMR spectrum of **$HC_2(BF_2L)C_2H$** in $CDCl_3$. The asterisks denote residual solvent signals.

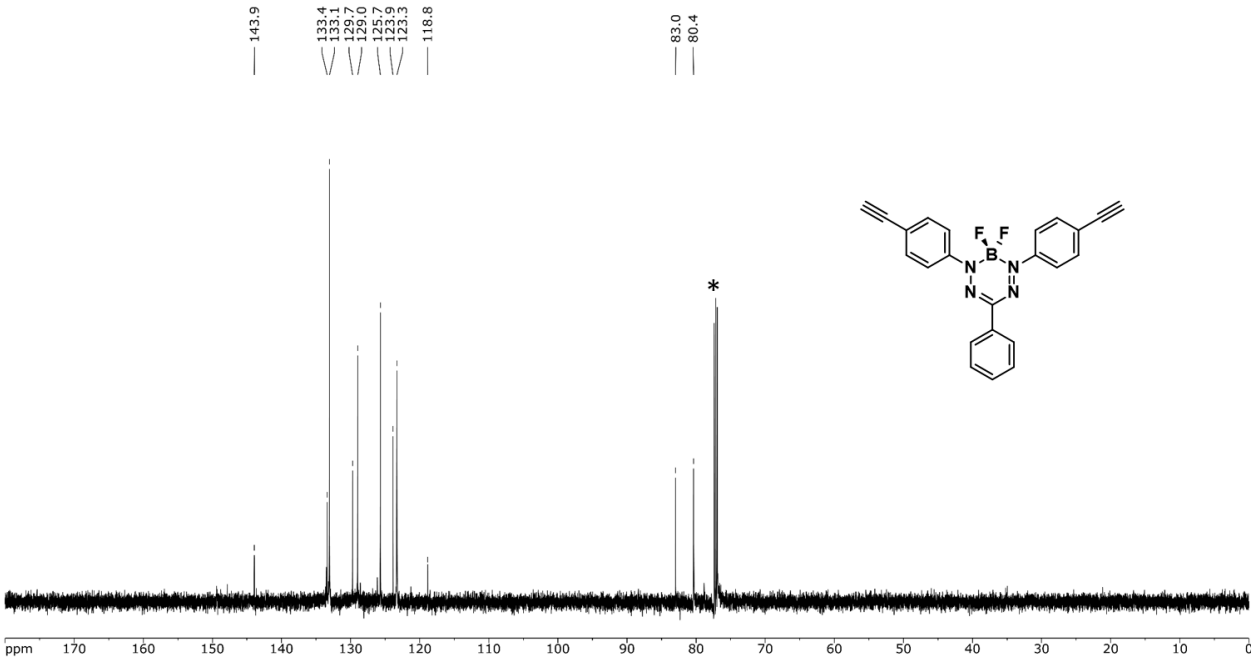

Fig. S10 $^{13}C\{^{1}H\}$ NMR spectrum of **$HC_2(BF_2L)C_2H$** in $CDCl_3$. The asterisk denotes solvent signal.

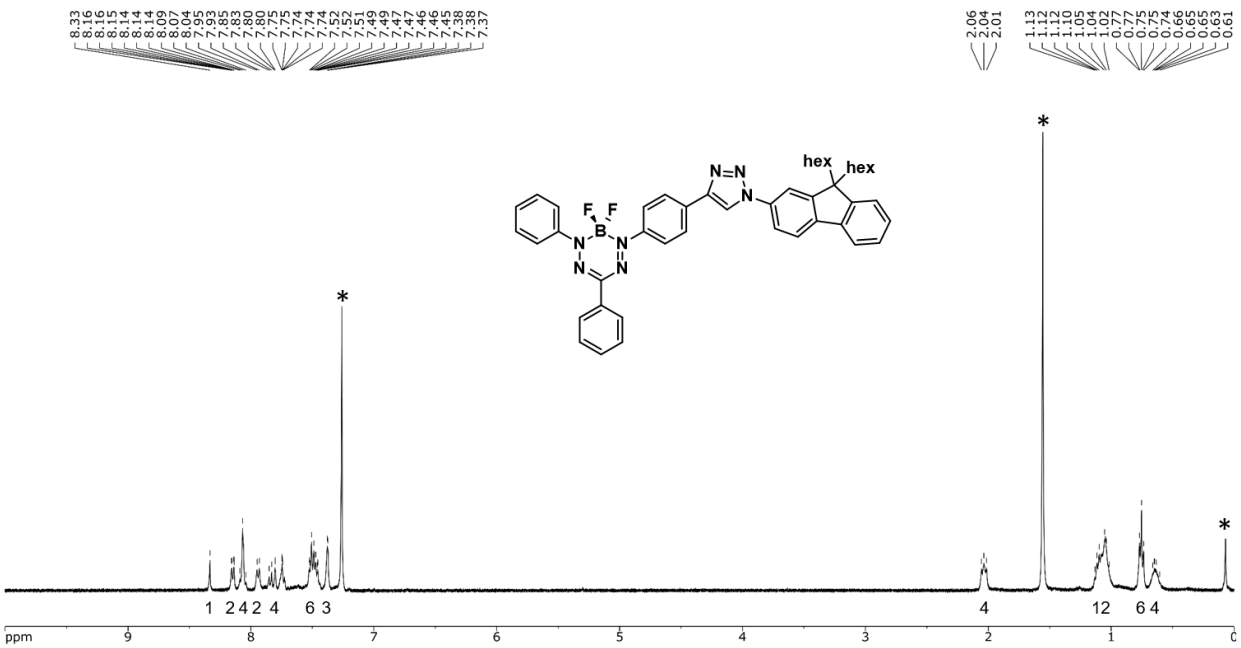

Fig. S11 ^{1}H NMR spectrum of **(BF_2L)-(hex$_2$Fl)** in $CDCl_3$. The asterisks denote residual solvent or grease signals.

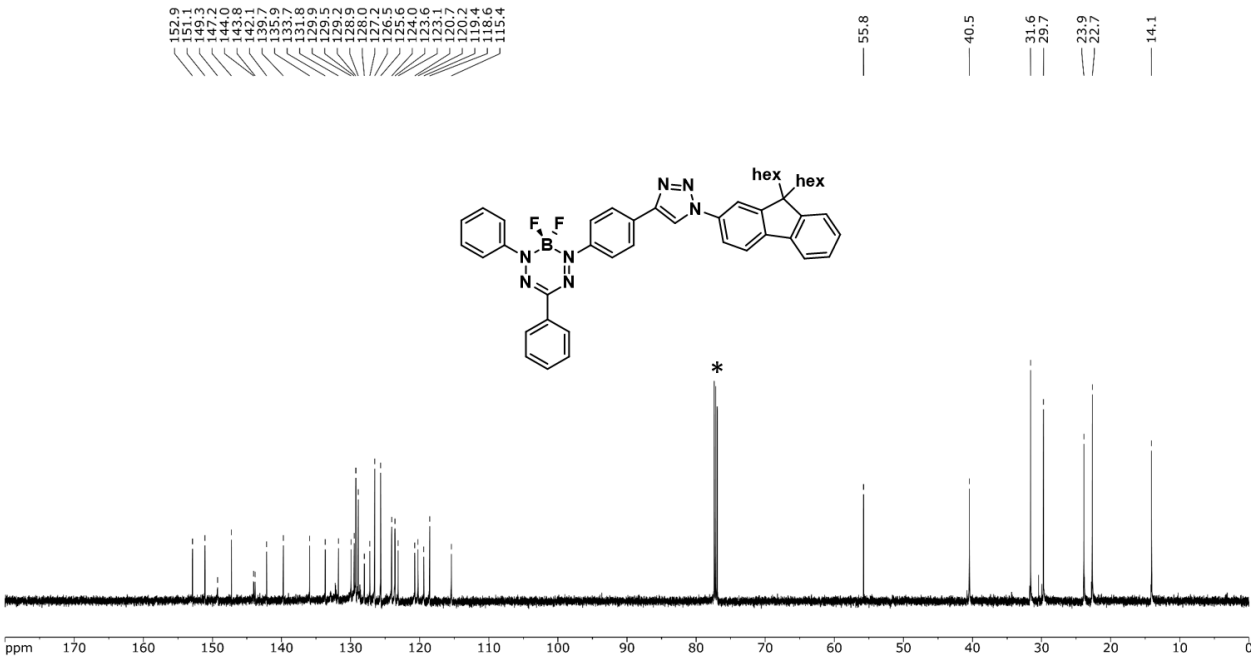

Fig. S12 $^{13}C\{^{1}H\}$ NMR spectrum of **(BF_2L)-(hex$_2$Fl)** in $CDCl_3$. The asterisk denotes solvent signal.

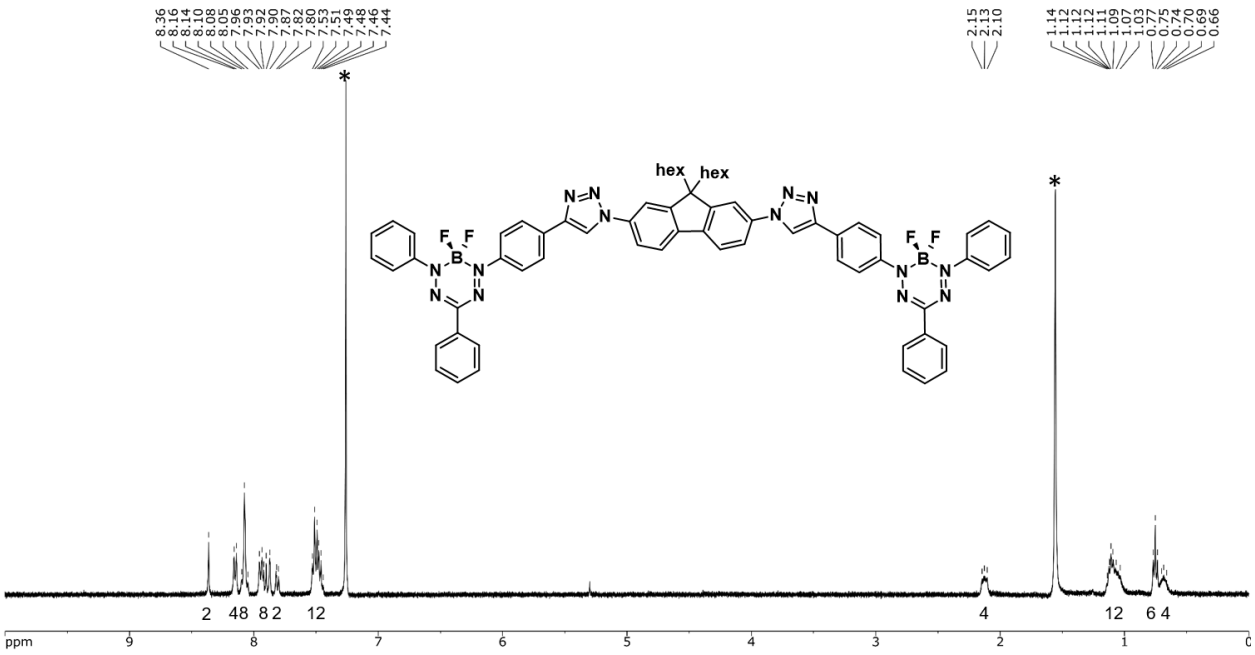

Fig. S13 ^{1}H NMR spectrum of **(BF$_2$L)-(hex$_2$Fl)-(BF$_2$L)** in $CDCl_3$. The asterisks denote residual solvent signals.

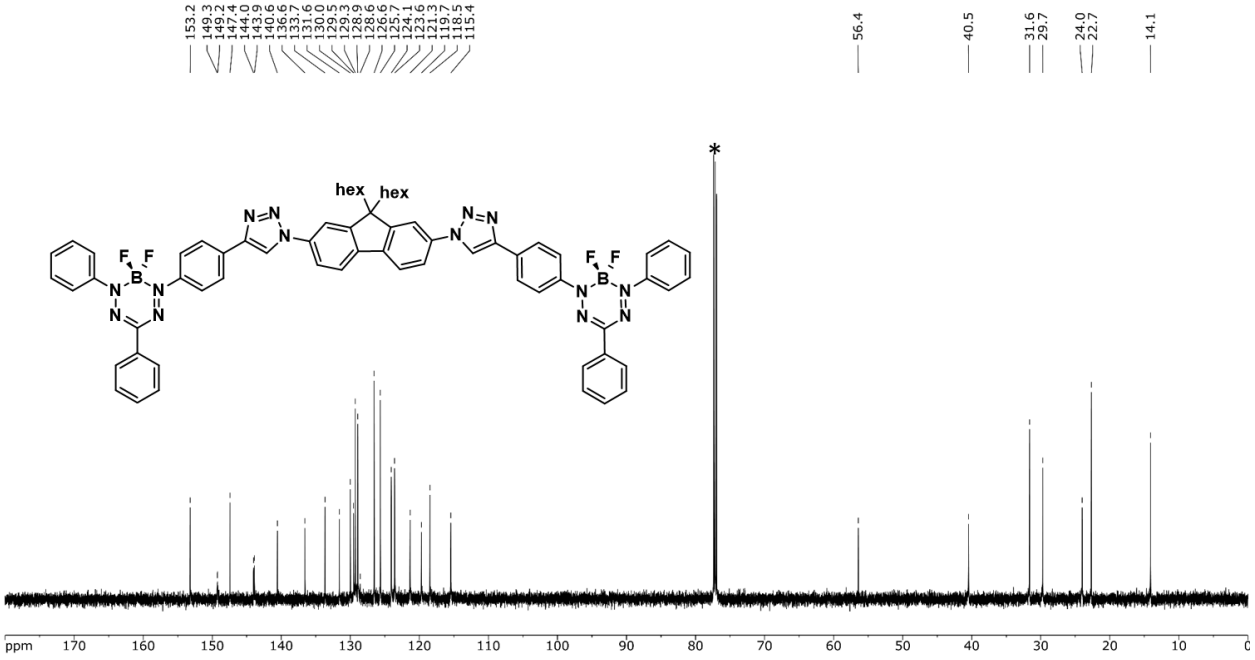

Fig. S14 $^{13}C\{^{1}H\}$ NMR spectrum of **(BF$_2$L)-(hex$_2$Fl)-(BF$_2$L)** in $CDCl_3$. The asterisk denotes solvent signal.

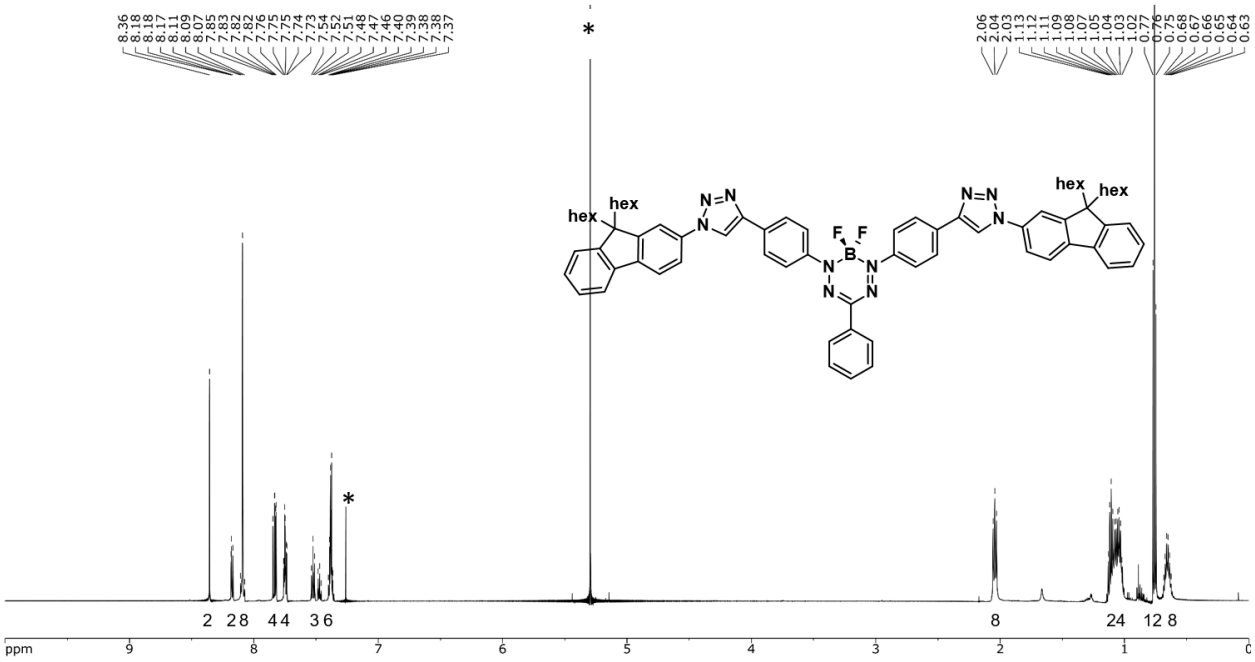

Fig. S15 ^{1}H NMR spectrum of **(hex$_2$Fl)-(BF$_2$L)-(hex$_2$Fl)** in $CDCl_3$. The asterisks denote residual solvent signals.

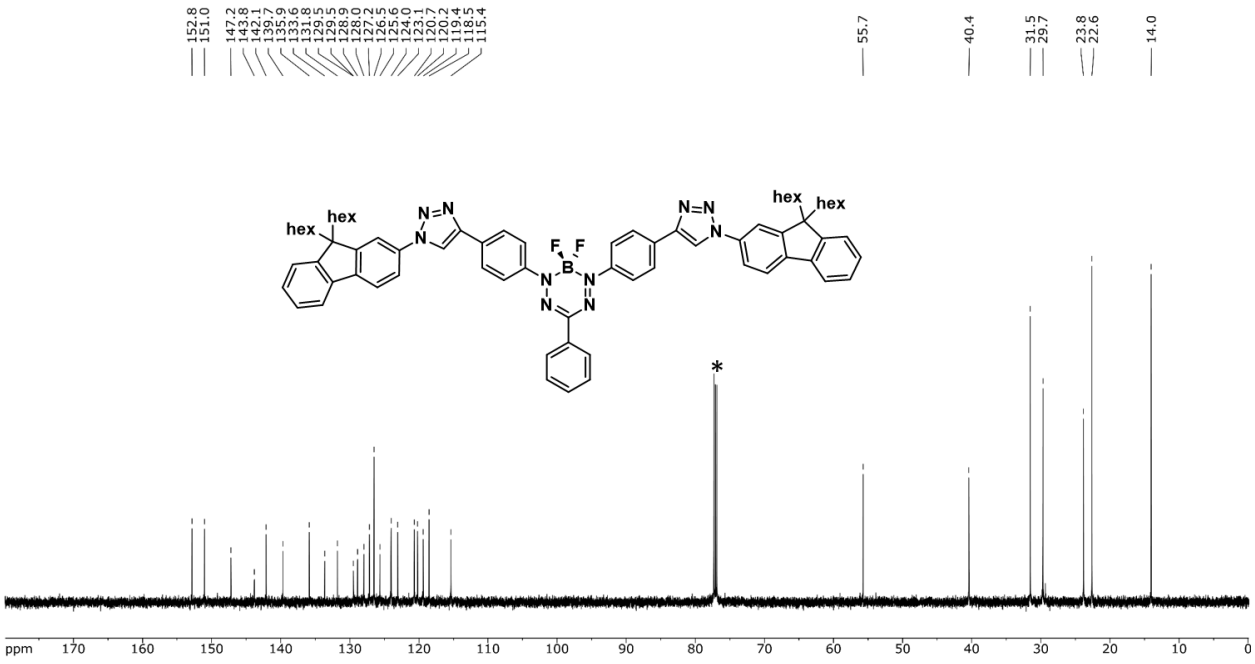

Fig. S16 $^{13}C\{^{1}H\}$ NMR spectrum of **(hex$_2$Fl)-(BF$_2$L)-(hex$_2$Fl)** in $CDCl_3$. The asterisk denotes solvent signal.

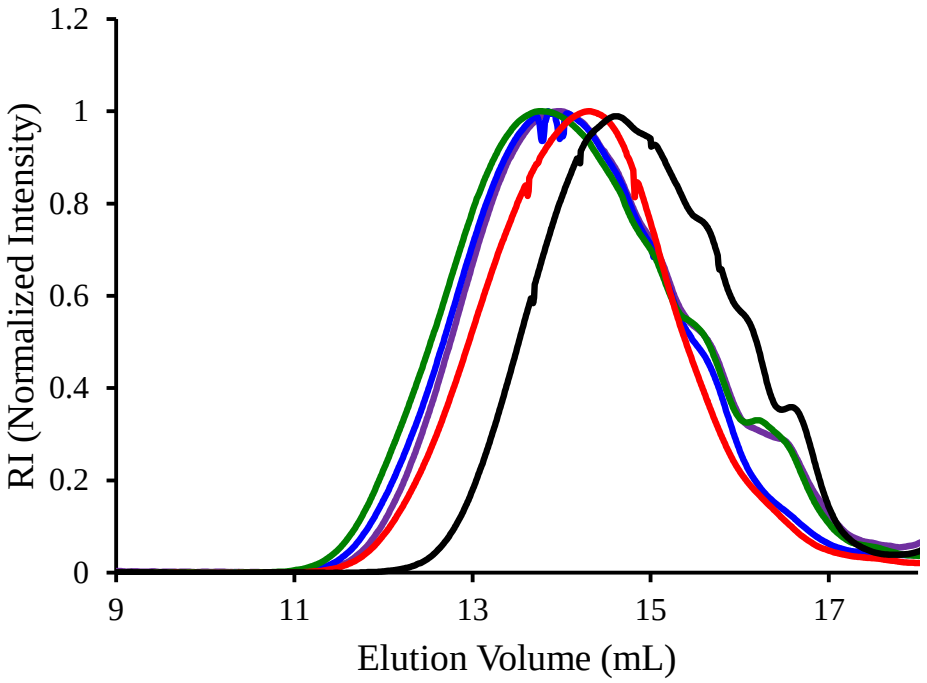

Fig. S17 GPC traces for aliquots of polymer **[(BF$_2$L)-(hex$_2$Fl)]$_n$** taken at 12 h (black), 24 h (purple), 48 h (blue), 72 h (green) and 168 h (red).

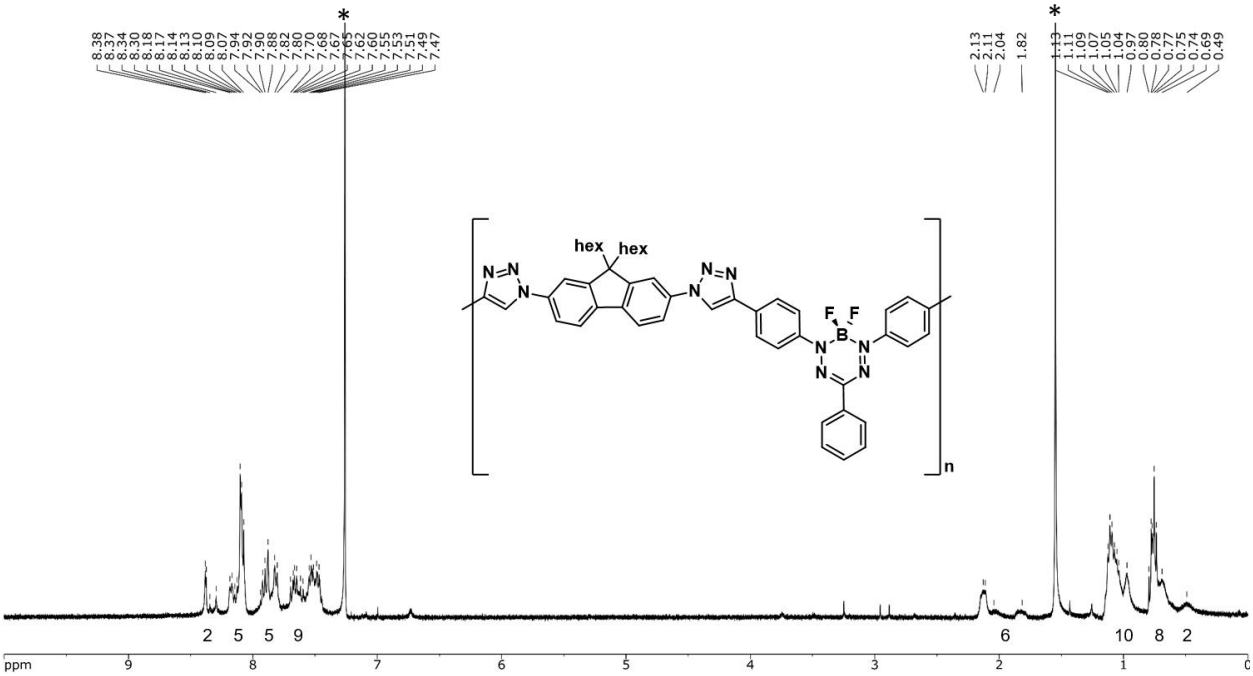

Fig. S18 ^{1}H NMR spectrum of **[(BF$_2$L)-(hex$_2$Fl)]$_n$** in $CDCl_3$. The asterisks denote residual solvent signals.

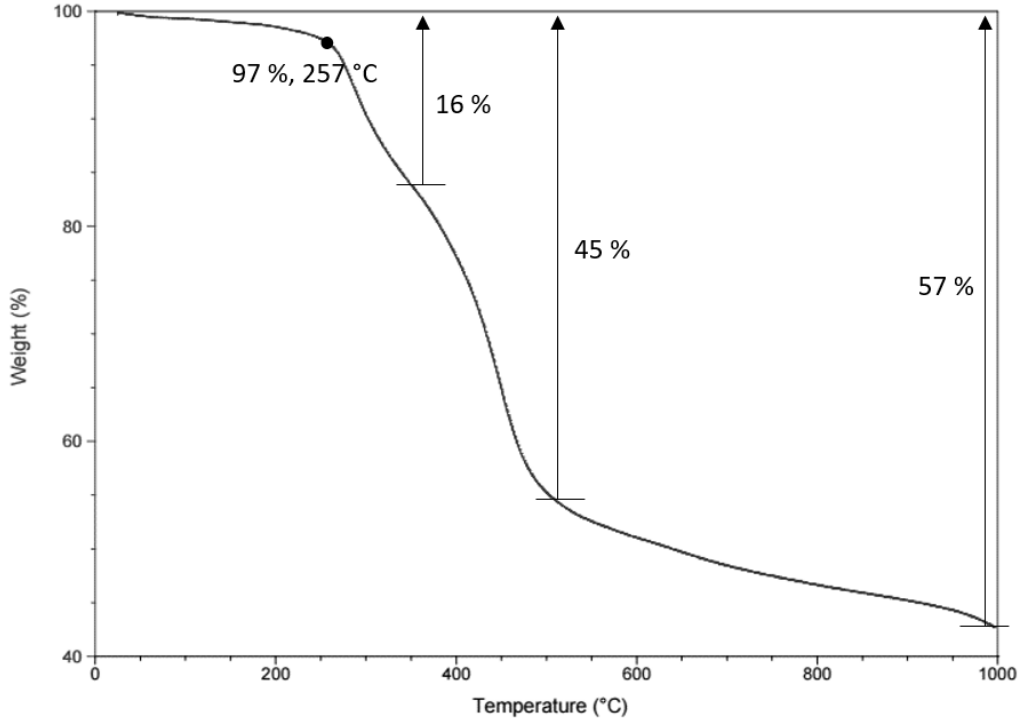

Fig. S19 TGA trace for **[(BF$_2$L)-(hex$_2$Fl)]$_n$**.

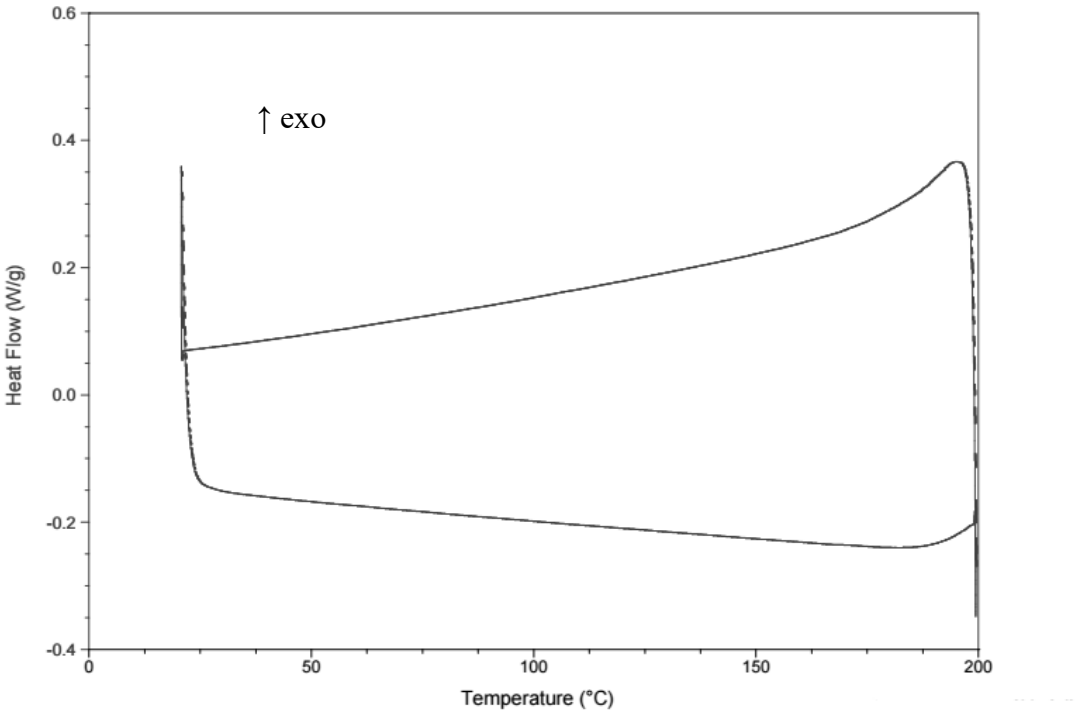

Fig. S20 DSC thermogram collected for **[(BF$_2$L)-(hex$_2$Fl)]$_n$**.

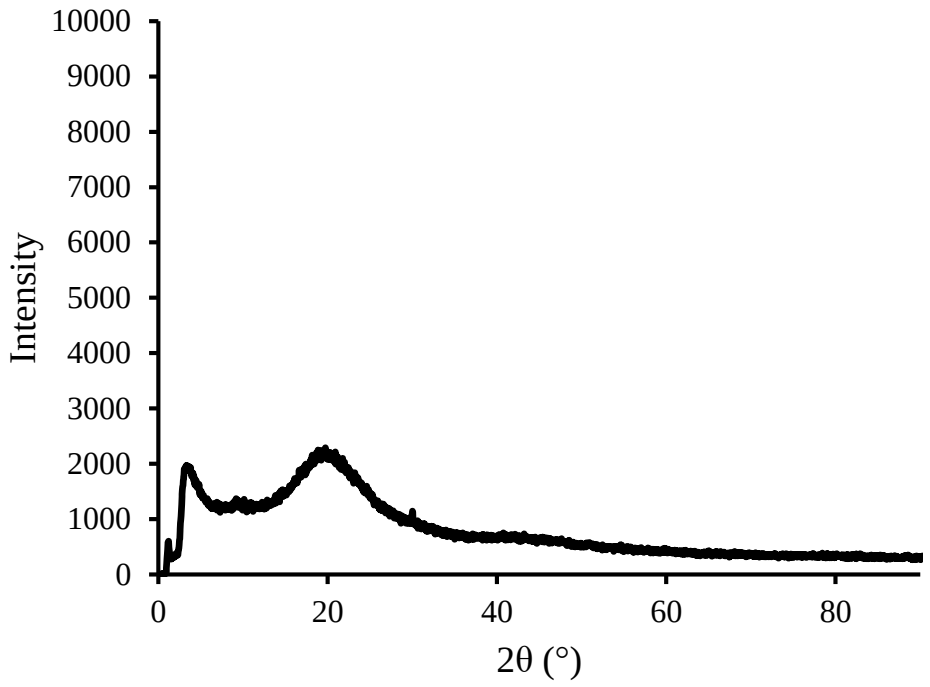

Fig. S21 Powder X-ray diffractogram for **[(BF$_2$L)-(hex$_2$Fl)]$_n$** collected on a glass slide.

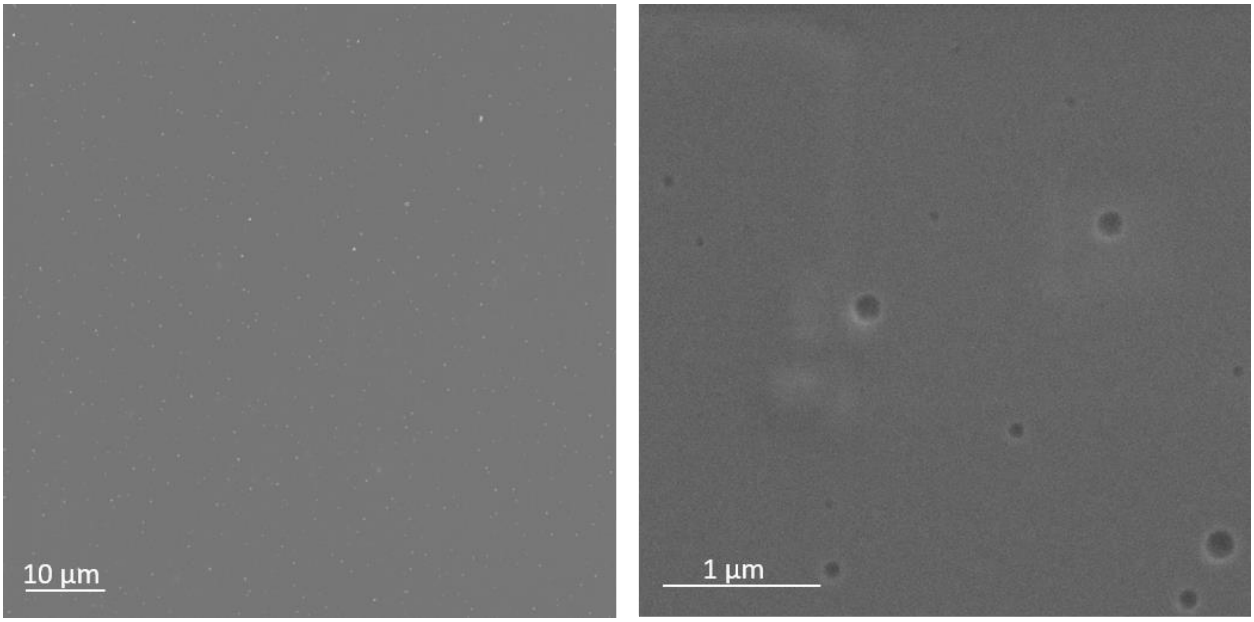

Fig. S22 SEM images of a thin film of **[(BF$_2$L)-(hex$_2$Fl)]$_n$** prepared from a chlorobenzene solution on a silicon wafer.

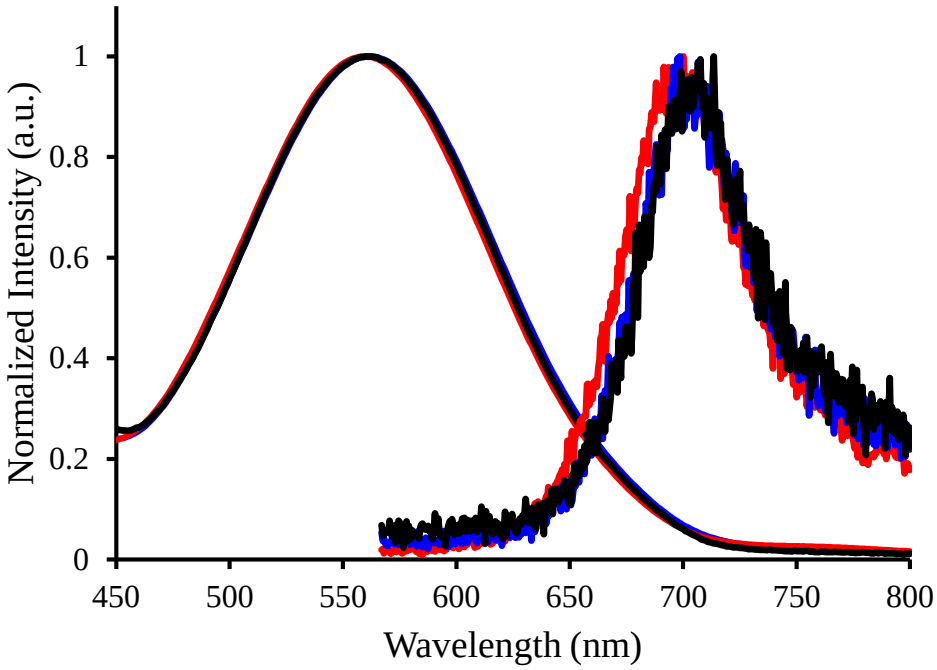

Fig. S23 Normalized UV-vis absorption and emission spectra of **[(BF$_2$L)-(hex$_2$Fl)]$_n$** with number average molecular weight of 6,000 g mol^{-1} (red), 10,000 g mol^{-1} (blue) and 17,000 g mol^{-1} (black) for 10^{-5} M DMF solution.

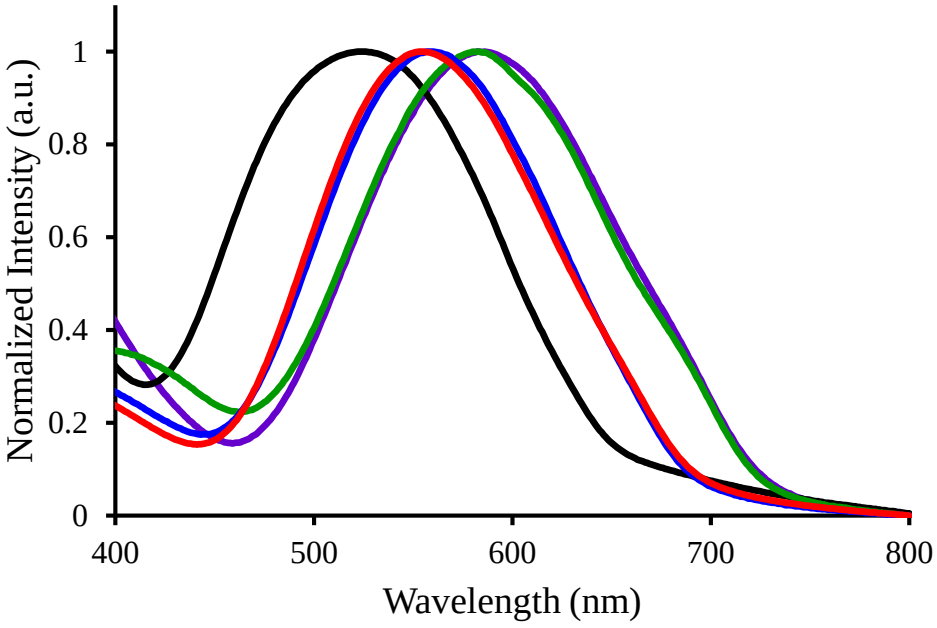

Fig. S24 Normalized thin-film UV-vis absorption spectra of **BF$_2$L** (black), **(BF$_2$L)-(hex$_2$Fl)** (red), **(hex$_2$Fl)-(BF$_2$L)-(hex$_2$Fl)** (green), **(BF$_2$L)-(hex$_2$Fl)-(BF$_2$L)** (blue), and **[(BF$_2$L)-(hex$_2$Fl)]$_n$** (purple).

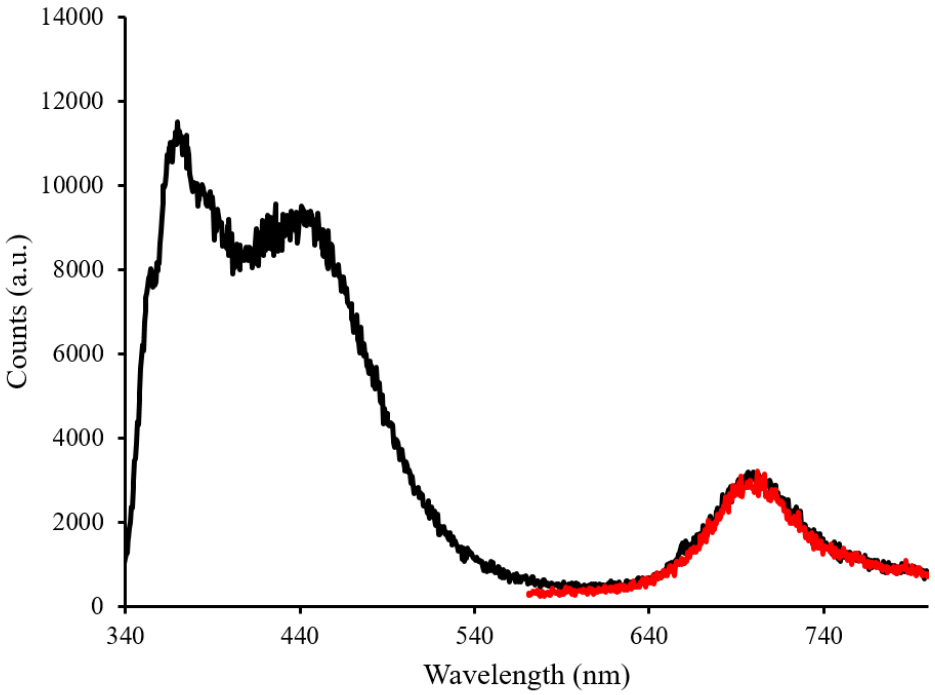

Fig. S25 Emission spectra of **[(BF$_2$L)-(hex$_2$F)]$_n$** recorded at excitation wavelength of 327 nm (black) and 557 nm (red) for a 10^{-5} M degassed DMF solution.

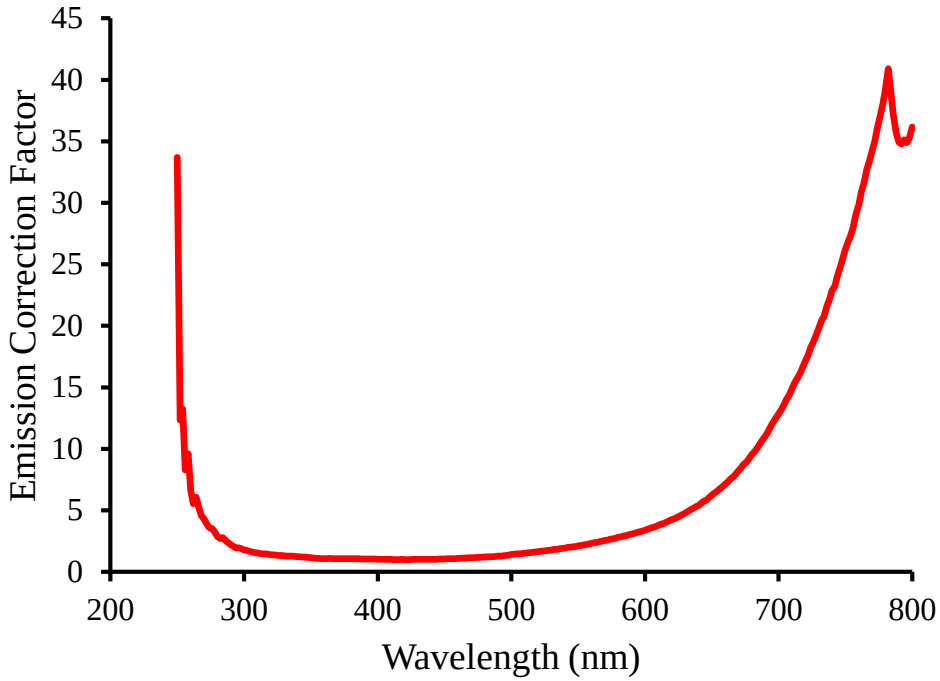

Fig. S26 Wavelength-dependent emission intensity correction provided by Photon Technology International.

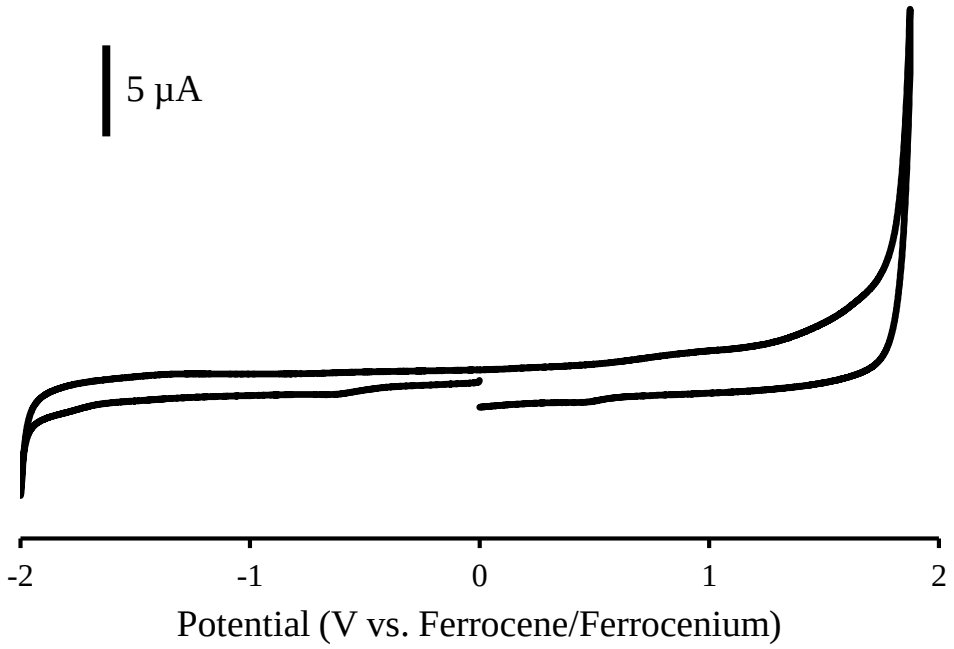

Fig. S27 Cyclic voltammogram of **hex$_2$Fl** recorded at 100 mV s^{-1} in a 1 mM DMF solution containing 0.1 M *n*Bu_4NPF_6 as supporting electrolyte.

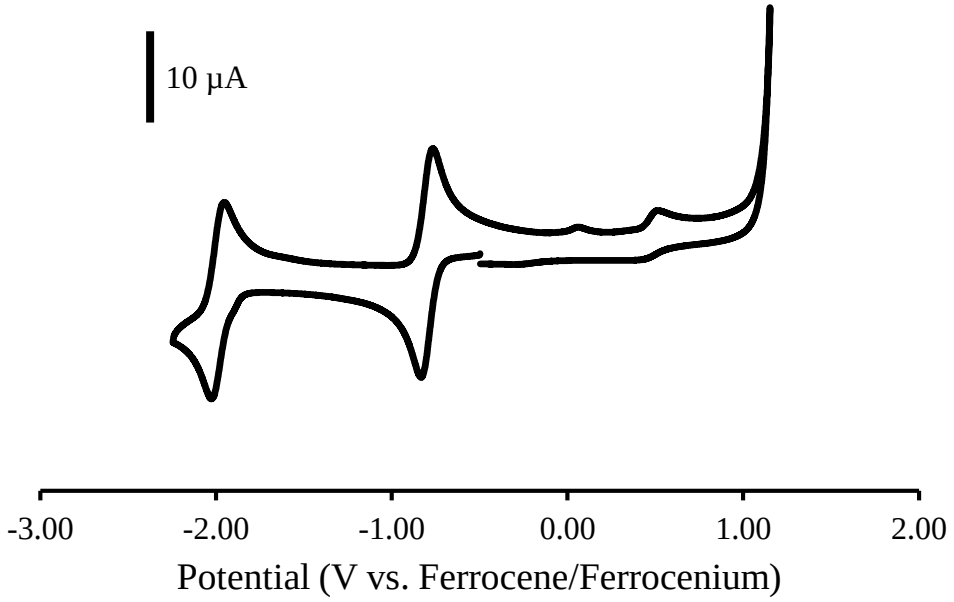

Fig. S28 Cyclic voltammogram of **BF_2L** recorded at 100 mV s^{-1} in a 1 mM DMF solution containing 0.1 M *n*Bu_4NPF_6 as supporting electrolyte.

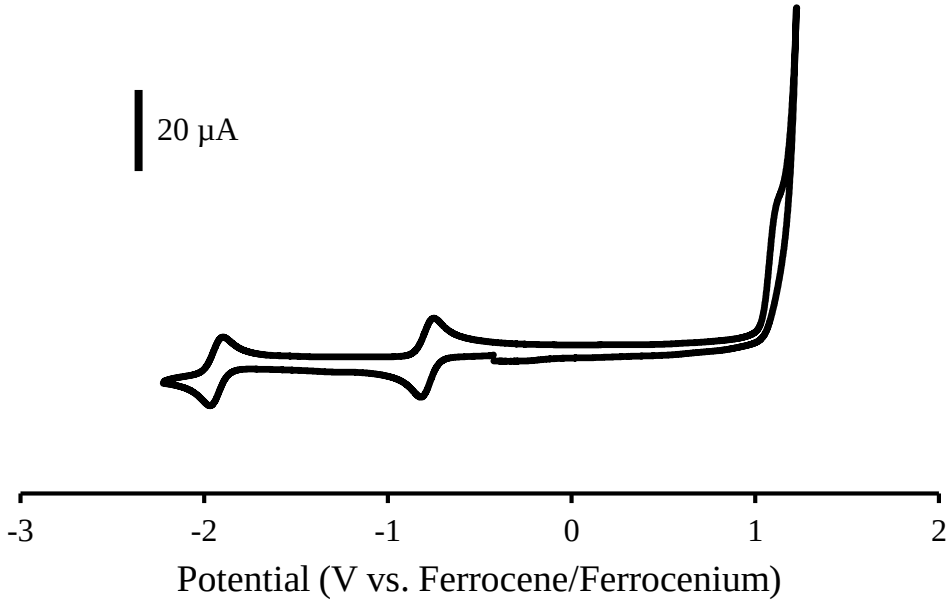

Fig. S29 Cyclic voltammogram of **(BF_2L)-(hex$_2$Fl)** recorded at 100 mV s^{-1} in a 1 mM DMF solution containing 0.1 M *n*Bu_4NPF_6 as supporting electrolyte.

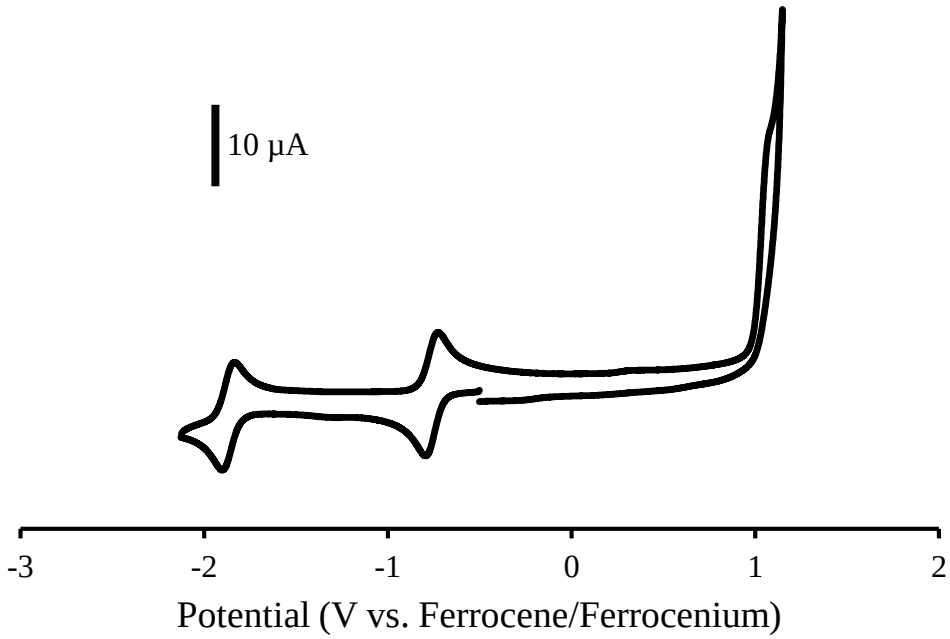

Fig. S30 Cyclic voltammogram of **(hex$_2$Fl)-(BF_2L)-(hex$_2$Fl)** recorded at 100 mV s^{-1} in a 1 mM DMF solution containing 0.1 M *n*Bu_4NPF_6 as supporting electrolyte.

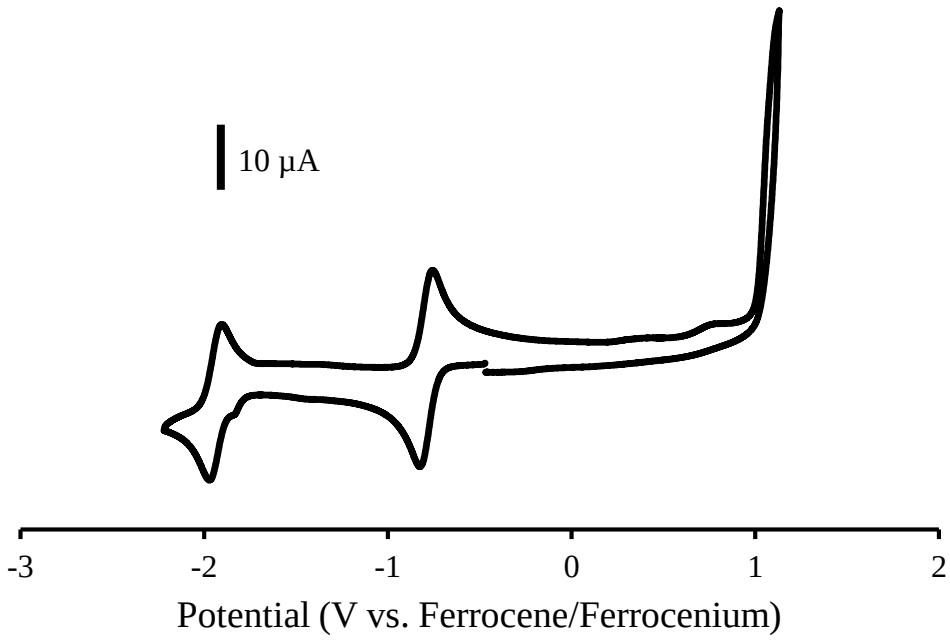

Fig. S31 Cyclic voltammogram of **(BF_2L)-(hex$_2$Fl)-(BF_2L)** recorded at 100 mV s^{-1} in a 1 mM DMF solution containing 0.1 M *n*Bu_4NPF_6 as supporting electrolyte.